STEM Real World Applications of Mathematics

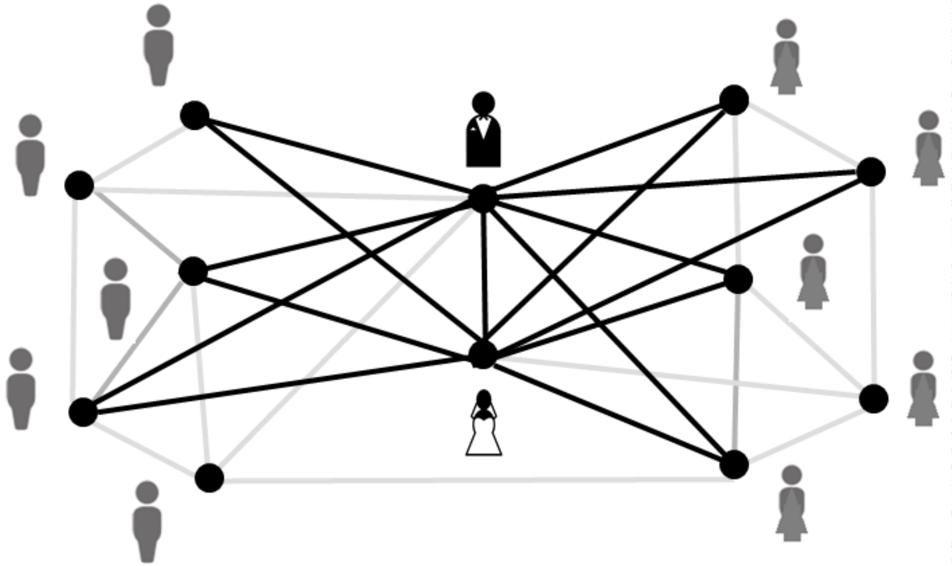

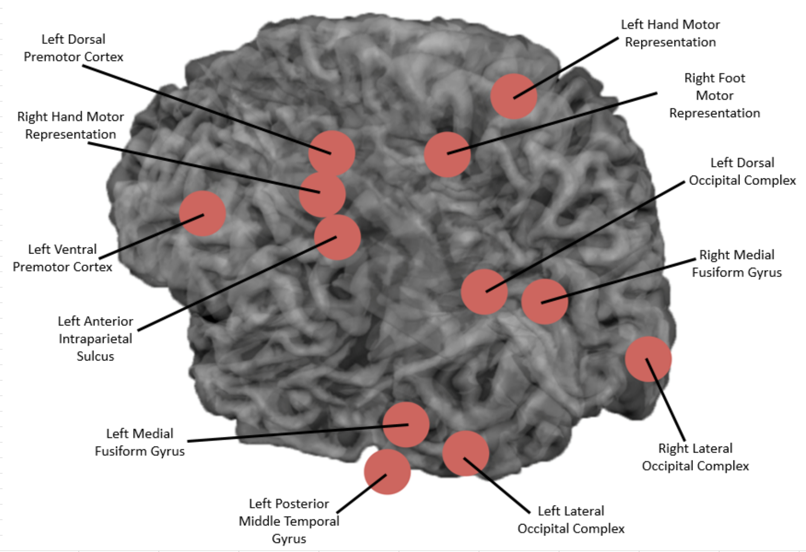

Darren A. Narayan
Rochester Institute of Technology

- Supported by NSF-CCLI STEM Real World Applications of Mathematics #1019532

Graph Theory

A graph is comprised of a set of vertices (dots) and edges (lines) where a line joins two vertices.

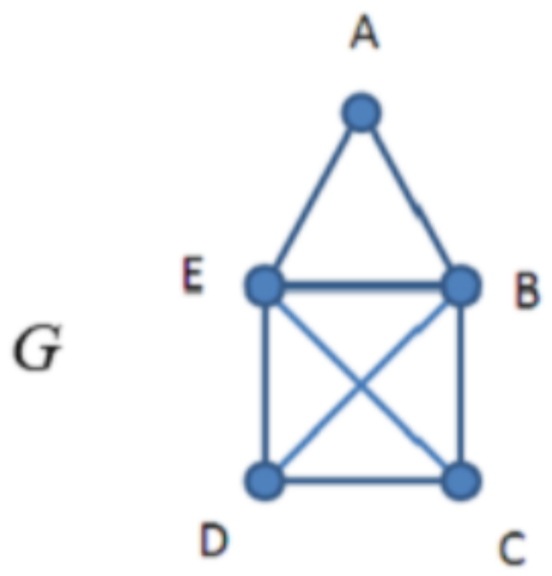

Graphs can be used to model social, biological, transportation, and other types of networks.

Which edges are the *most central* in a graph?

“Local closed neighborhoods”

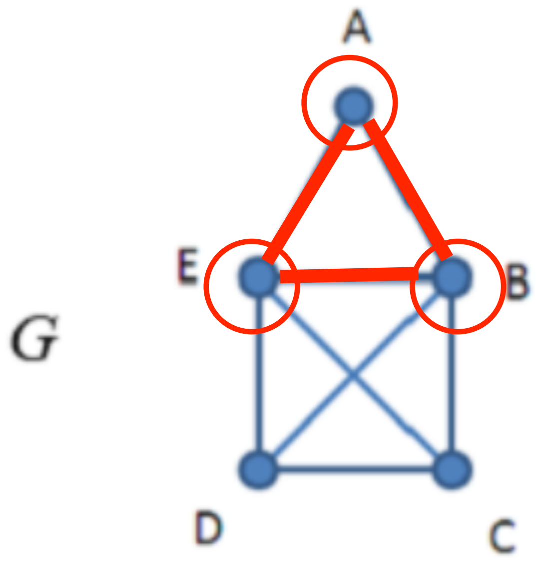

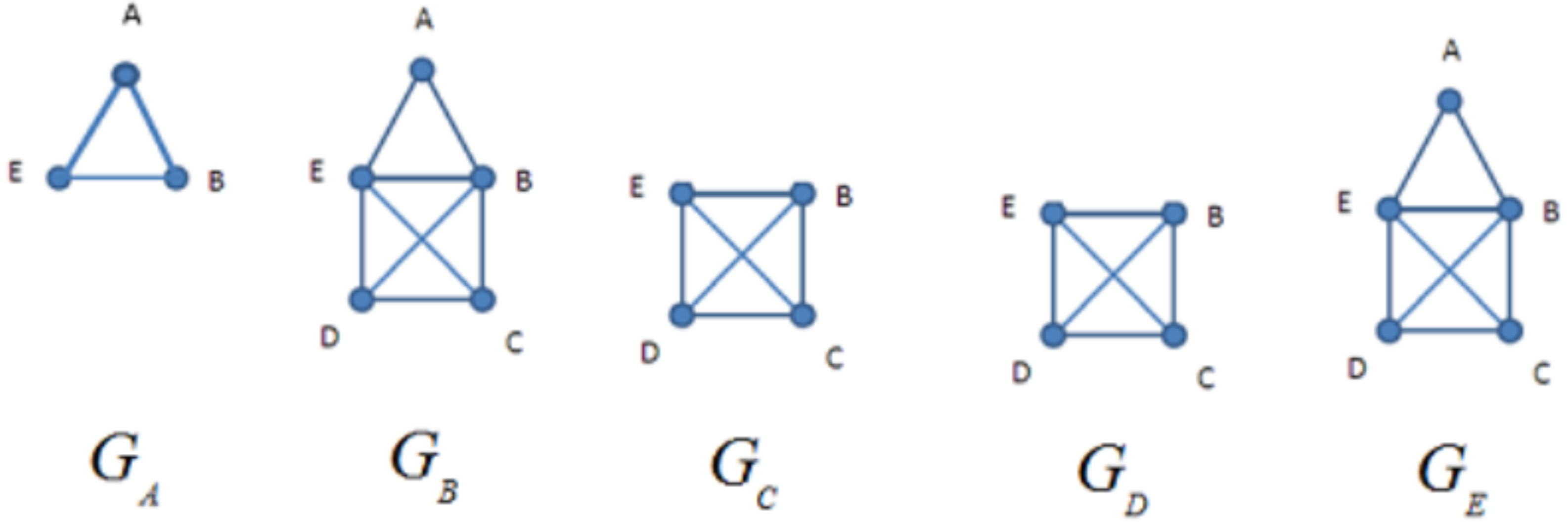

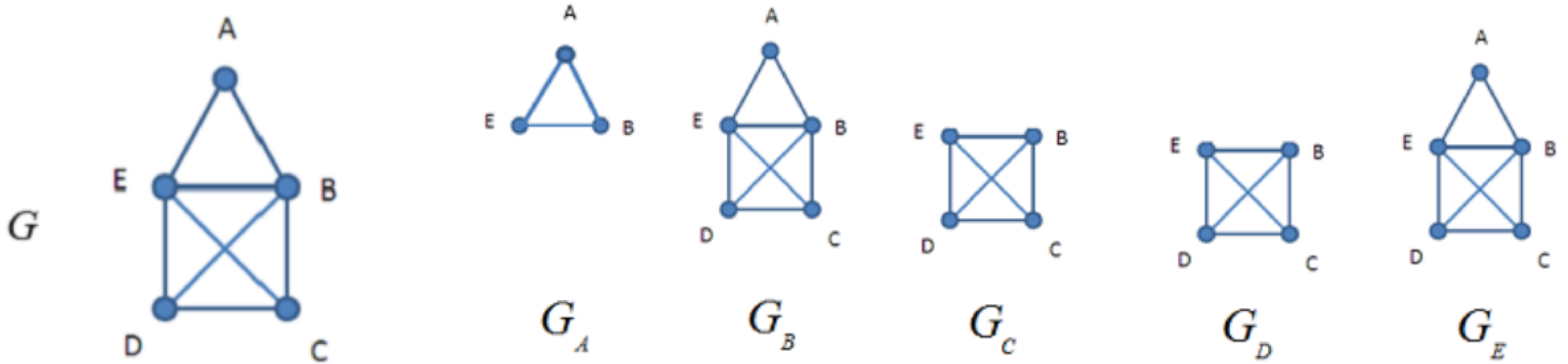

The number of subgraphs in which each edge appears:

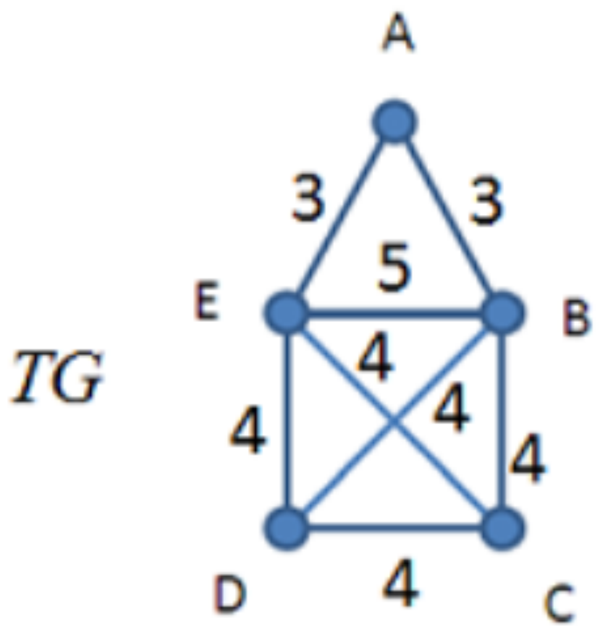

“Clustering Centrality”

- Clustering centrality can be linked to a problem in structural graph theory.

- A common problem in structural graph theory is:

Given a graph *G* determine a largest sized particular subgraph *H*.

  - In our case *H* will be a “book graph”.

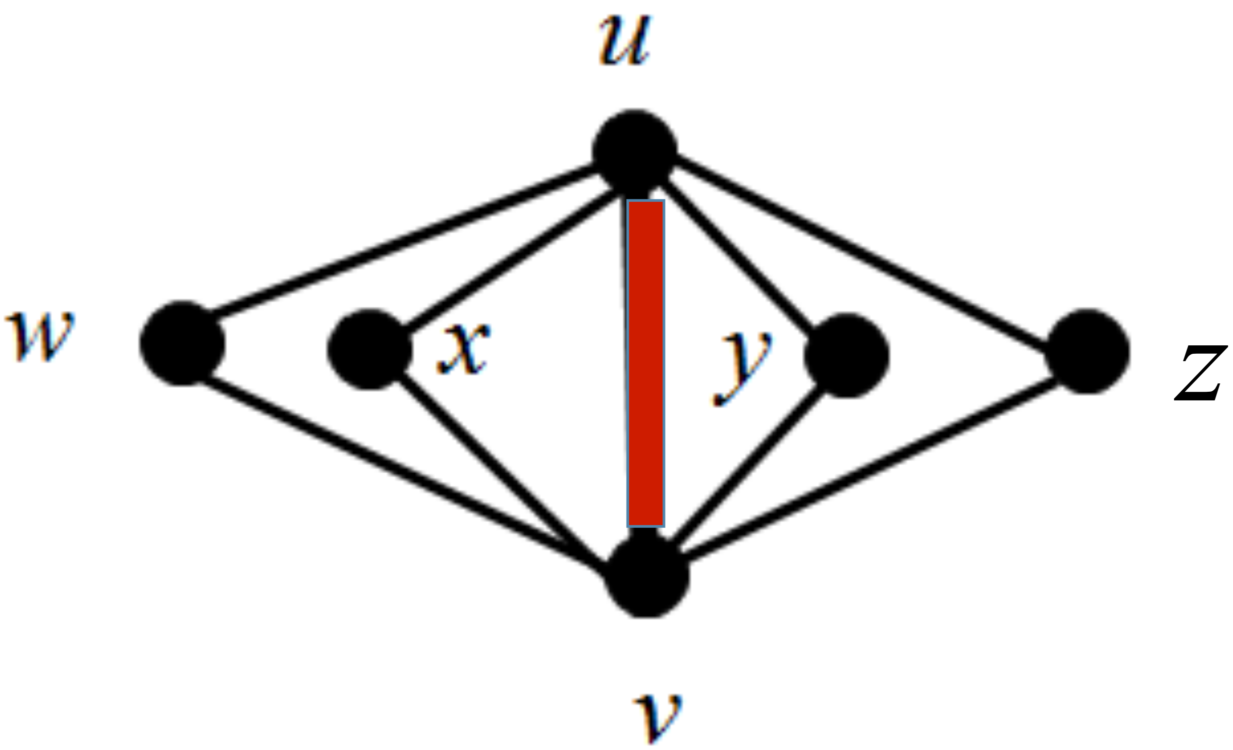

Applications

Analysis of functional MRI data

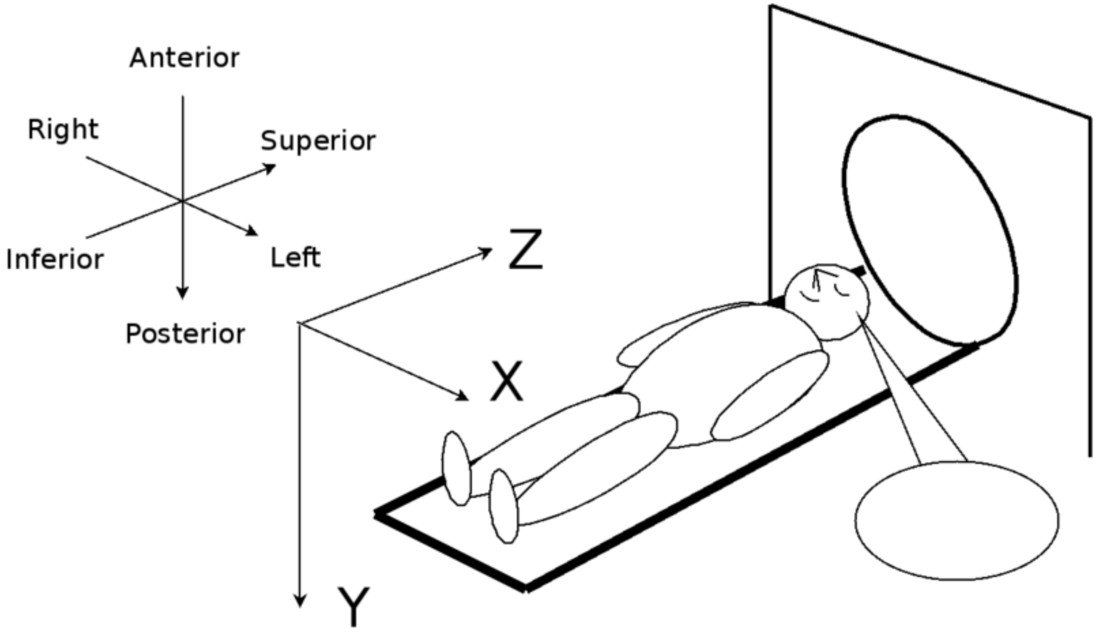

From Brains to Graphs

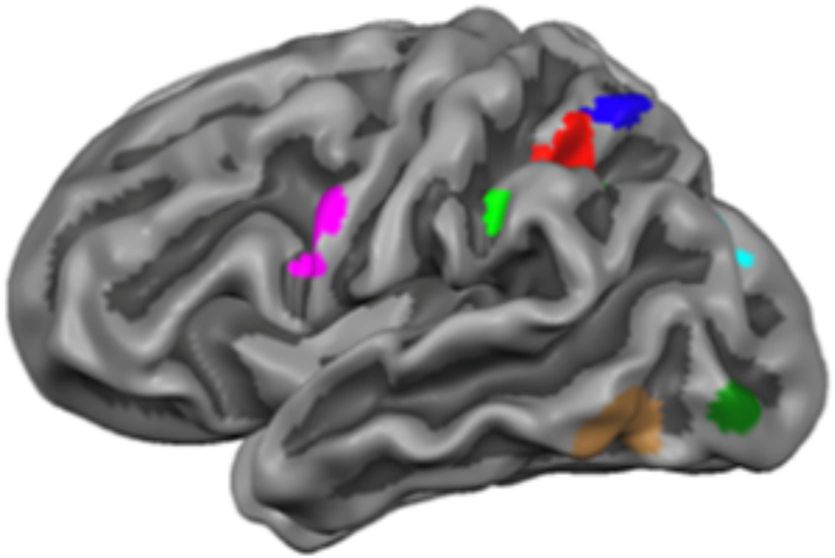

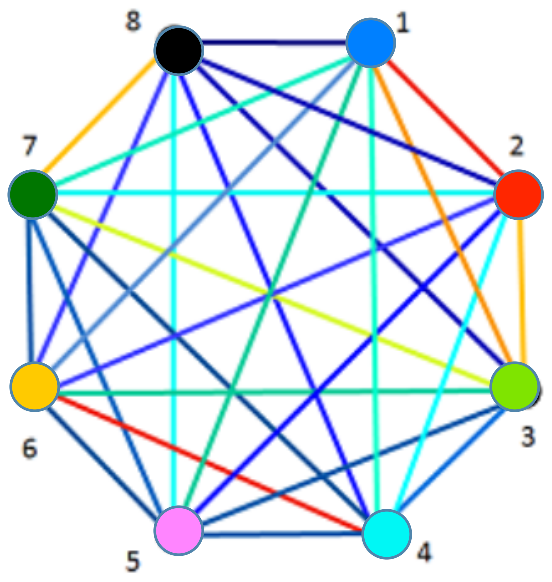

In our study we will use graph theory to model the brain. The vertices will represent regions of the brain (Talairach defined) and edges will represent *functional* connections between the regions.

We monitor oxygen levels in the blood over the length of a scan.

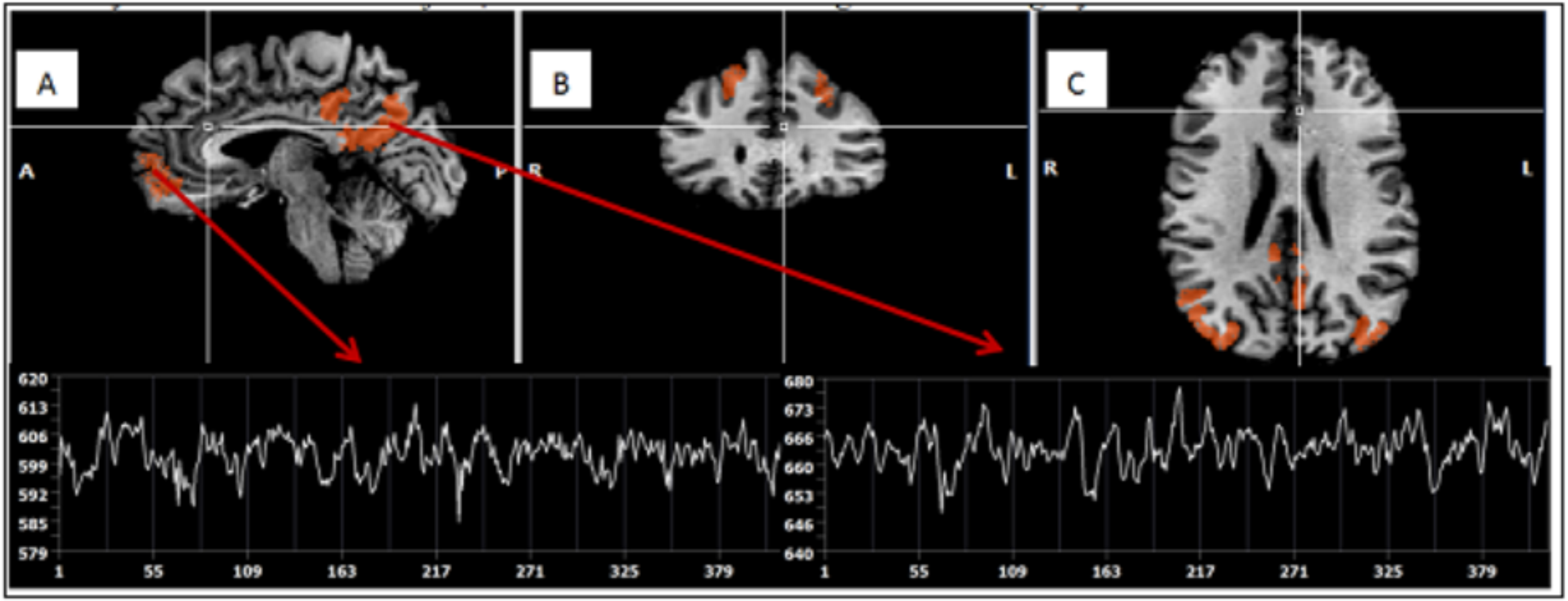

Images from E. B. Hintz, URMC

- We used clustering centrality to analyze networks arising from functional MRI data from the Rochester Center for Brain Imaging.

- In the research study 12 subjects were asked to undergo functional MRI scans where they would view and pantomime various tools (hammer, scissors, screwdriver, knife, pliers, corkscrew).
  (All subjects were right-handed).

- We looked at correlations between the blood oxygen levels between each pair of 12 different regions. A two sided t test was performed and statistically significant values ($t > 2.75$) were selected.

- We then created two networks:
  (i) pantomiming was greater than viewing
  (ii) viewing greater than pantomiming

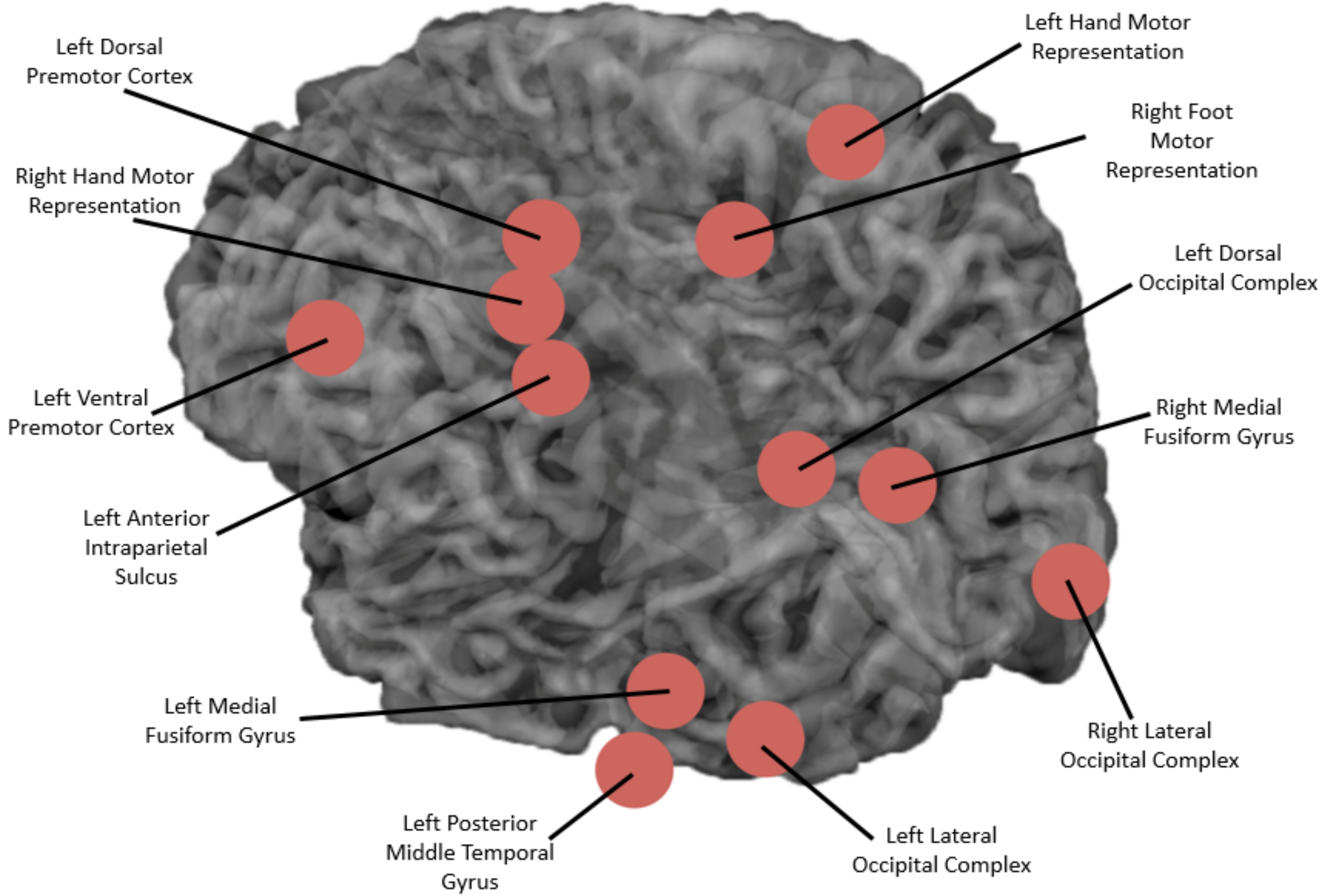
Left Dorsal Premotor Cortex
Right Hand Motor Representation
Left Ventral Premotor Cortex
Left Anterior Intraparietal Sulcus
Left Medial Fusiform Gyrus
Left Posterior Middle Temporal Gyrus
Left Lateral Occipital Complex
Left Hand Motor Representation
Right Foot Motor Representation
Left Dorsal Occipital Complex
Right Medial Fusiform Gyrus
Right Lateral Occipital Complex

Clustering Centrality: Pantomiming Greater than Viewing -The Network.

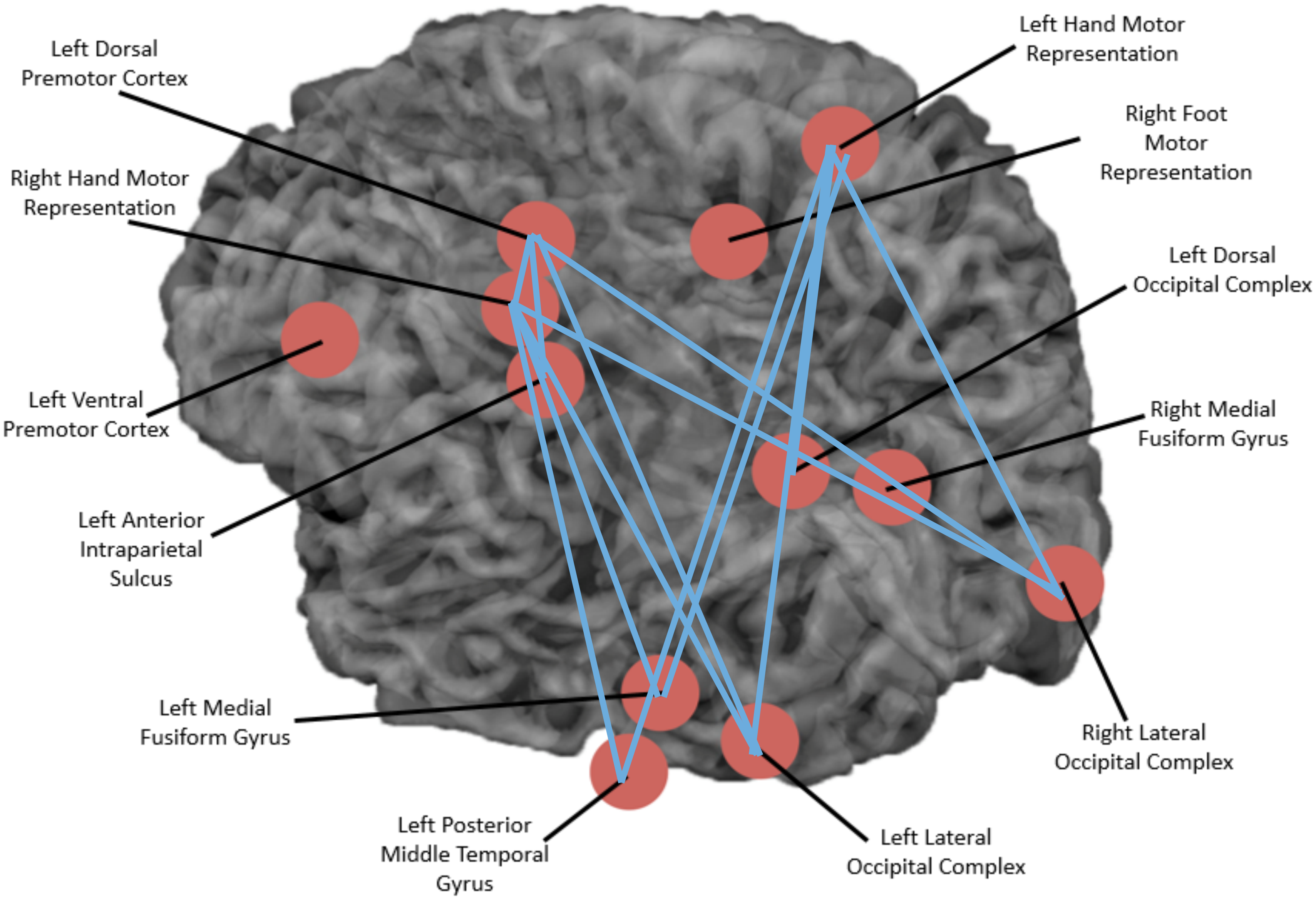

Clustering Centrality: Pantomiming Greater than Viewing

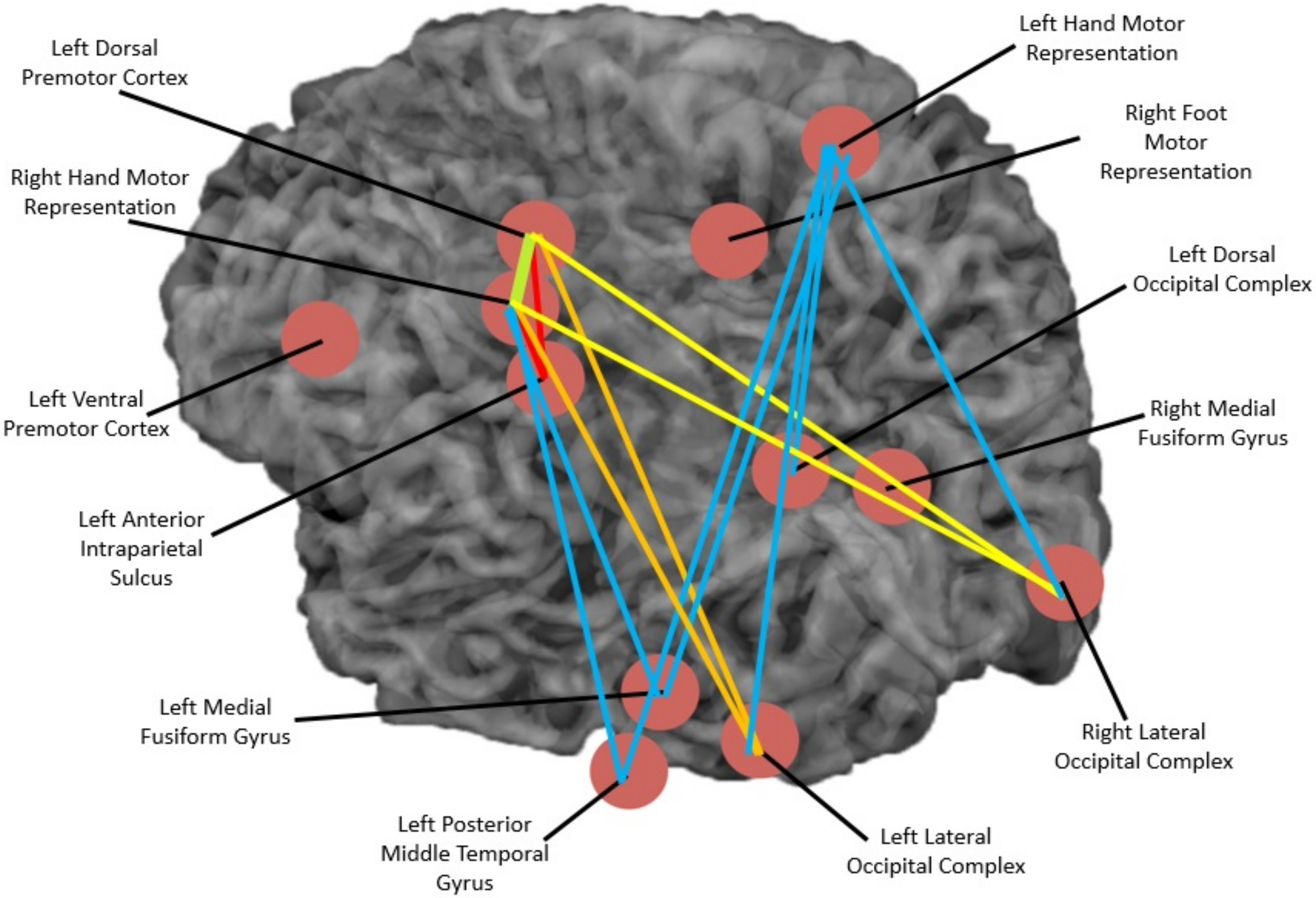

Clustering Centrality: Viewing Greater than Pantomiming

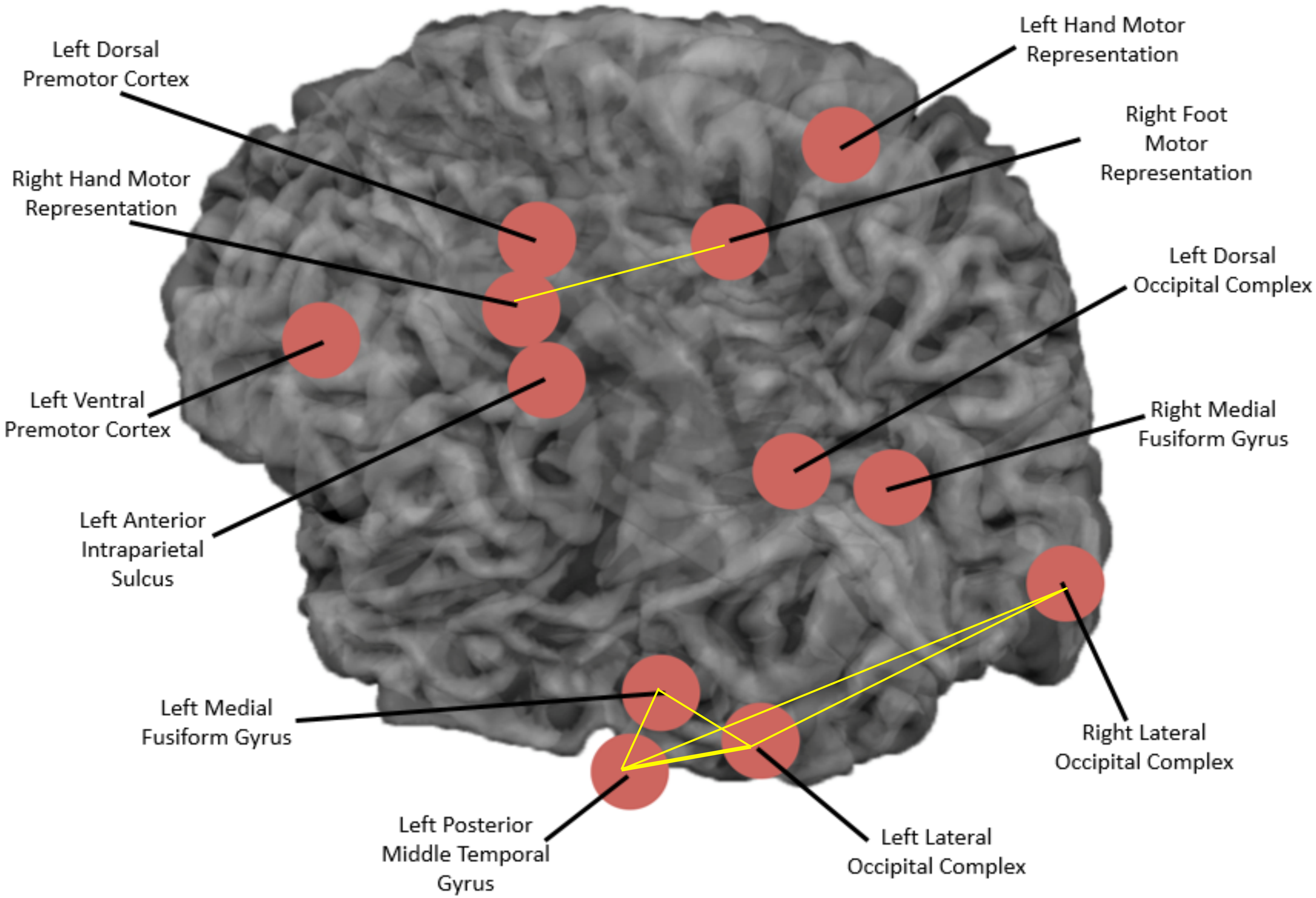

When pantomiming > viewing the *motor* regions show increased correlations.

When viewing > pantomiming the *visual* regions shown increased correlations.

Graphs and Social Networks

We can also use a graph to represent relationships among attendees at a wedding.

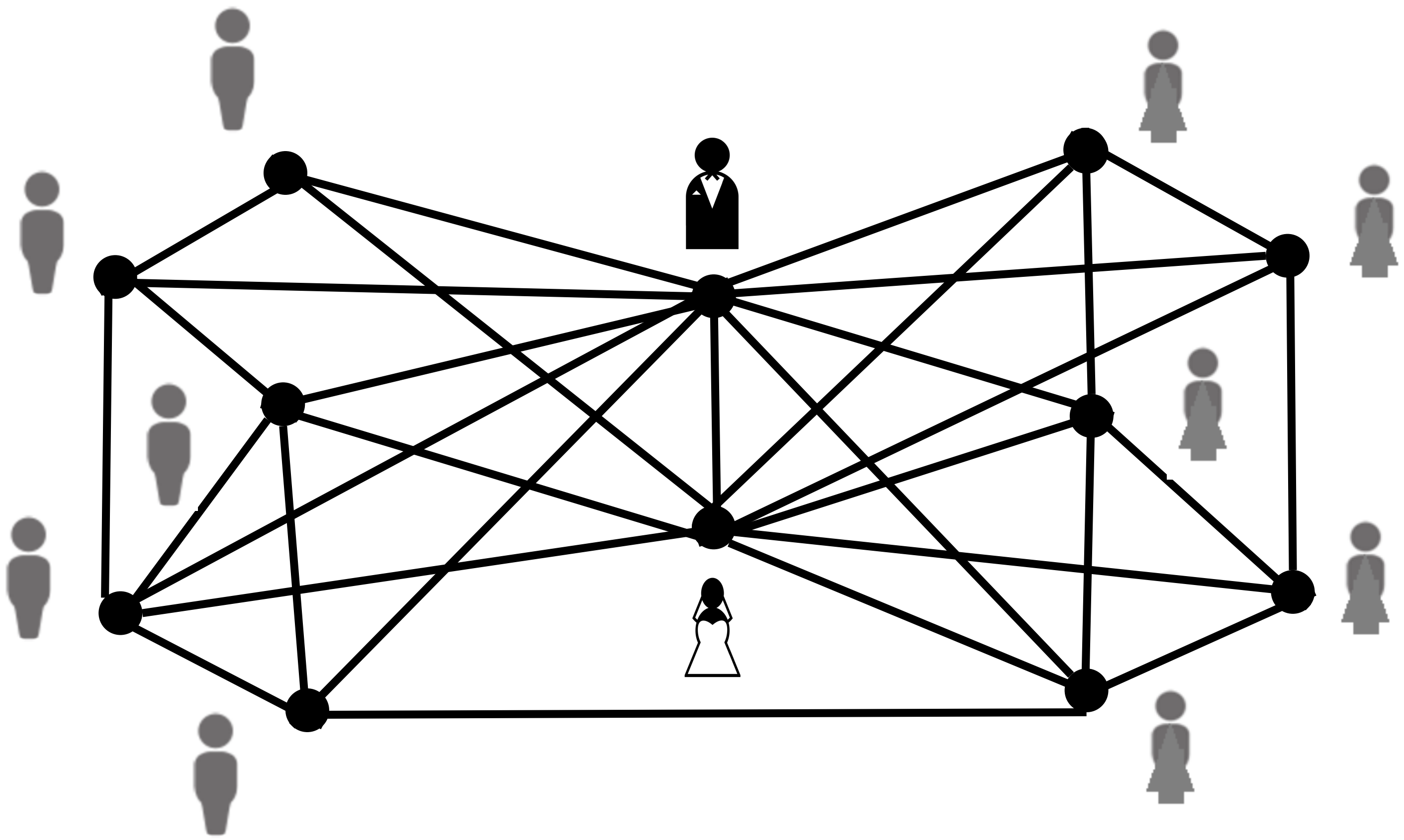

We note that in this network that everyone knows the bride or the groom (or both).

However suppose we want to see who is best connected to *both* the bride and the groom.

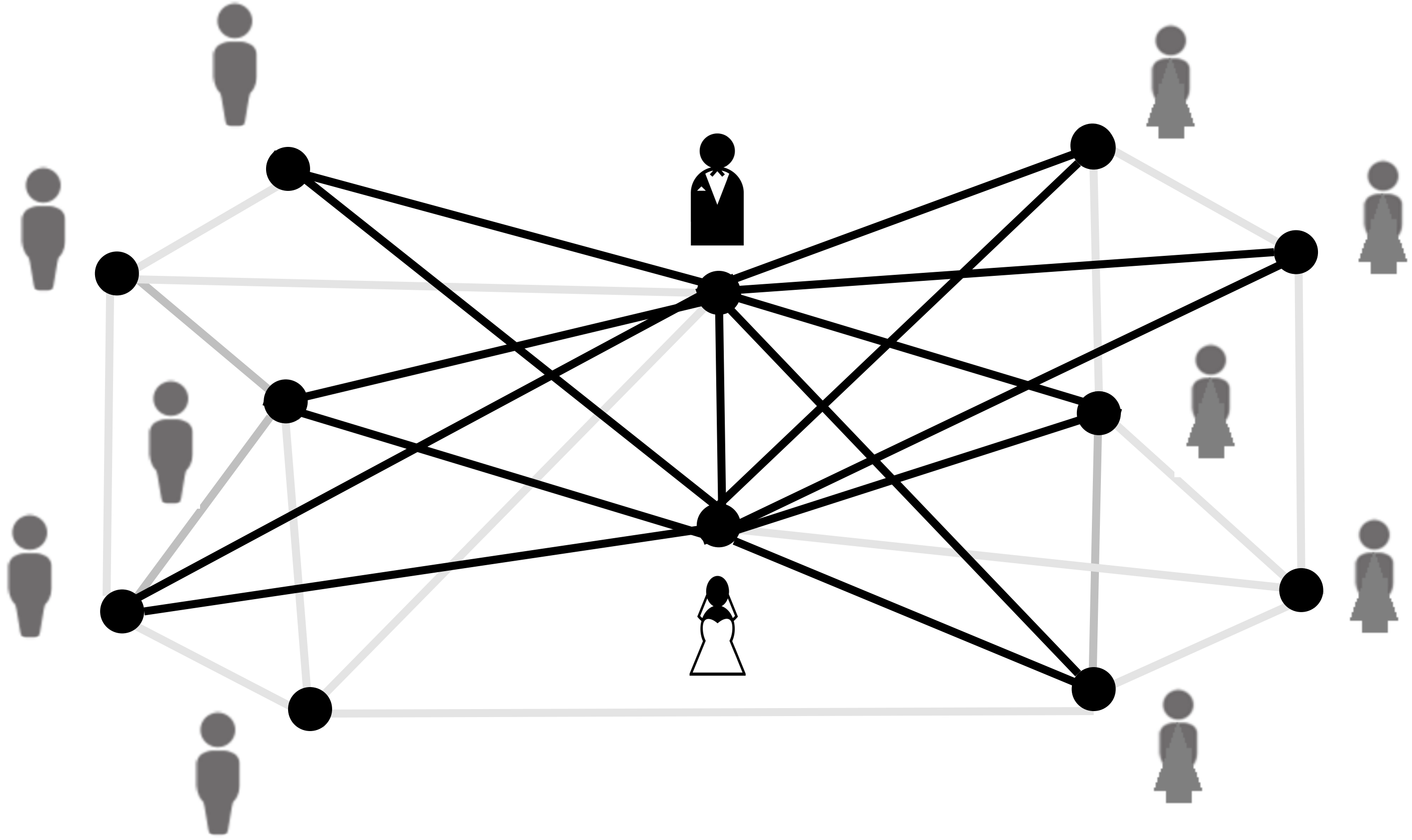

FASHION & STYLE

The Power of Two

Power Couples on Twitter and Instagram

By ALEX WILLIAMS AUG. 13, 2014

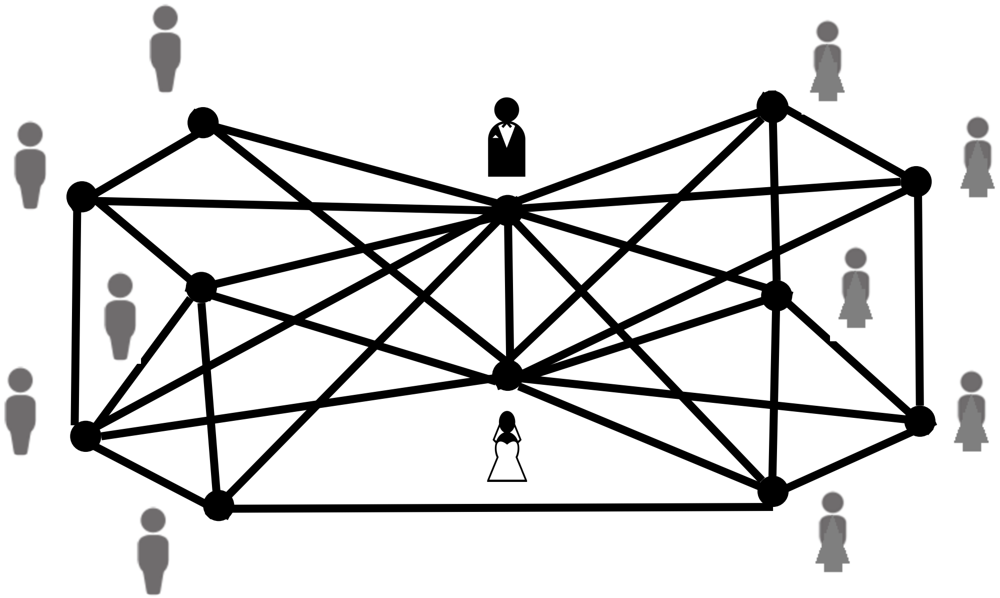

What happens to the topology of the network when two vertices are merged?

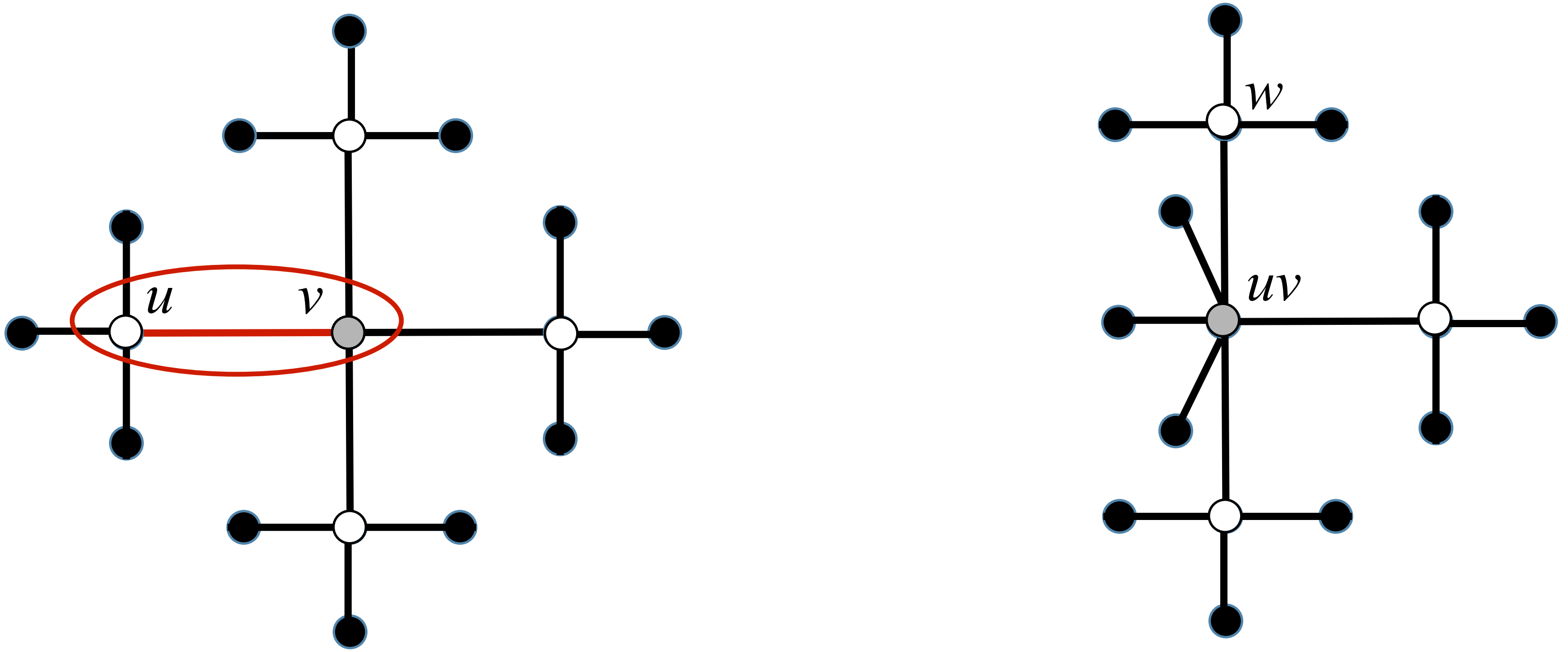

This problem could be studied using data from social media networks.

R. Lopez, J. Worrell, R. Florez, and D. A. Narayan, *Edge Contraction and Betweenness Centrality*, to be submitted for publication.

Brain connectivity and Traumatic Brain Injuries in Athletes

Charities

A study involved 10 football players that received DTI scans before and after the season.

Helmets were outfitted with linear accelerometers with the Head Impact Telemetry System (HITS).

Each impact to the helmet is measured with both linear and rotational acceleration.

Repetitive sub-concussive head hits (RSH) (incurred during sports, military duty, and alike) produce changes in brain white matter (WM) that may contribute to the development or progression of chronic traumatic encephalopathy (CTE) later in life.

Research studies have shown an inconsistent relationship between acute brain WM changes and the total number and magnitude of RSHs over a season of play.

Prior research has not accounted for the interval of time between hits (TBH) or the period of time between an impact and the assessment (e.g. diffusion tensor imaging; DTI) (TUA).

Frequency of exposures or time between RSHs, as well as timing of exposure relative to measuring the outcome (TUA), is likely to influence brain WM changes.

10 collegiate football players at the University of Rochester

Parameter	Mean	(SD)
Age (years)	20.4	(1.08)
Body Mass Index (kg/m^2)	30.74	(1.58)

Position	Total Head Hits
Running Back	431
Tight End	572
Linebacker	612
Defensive Line	617
Defensive Line	649
Full Back	1,042
Linebacker	1,142
Defensive Line	1,423
Offensive Tackle	1,431
Center	1,850

doi:10.1371/journal.pone.0094734.t002

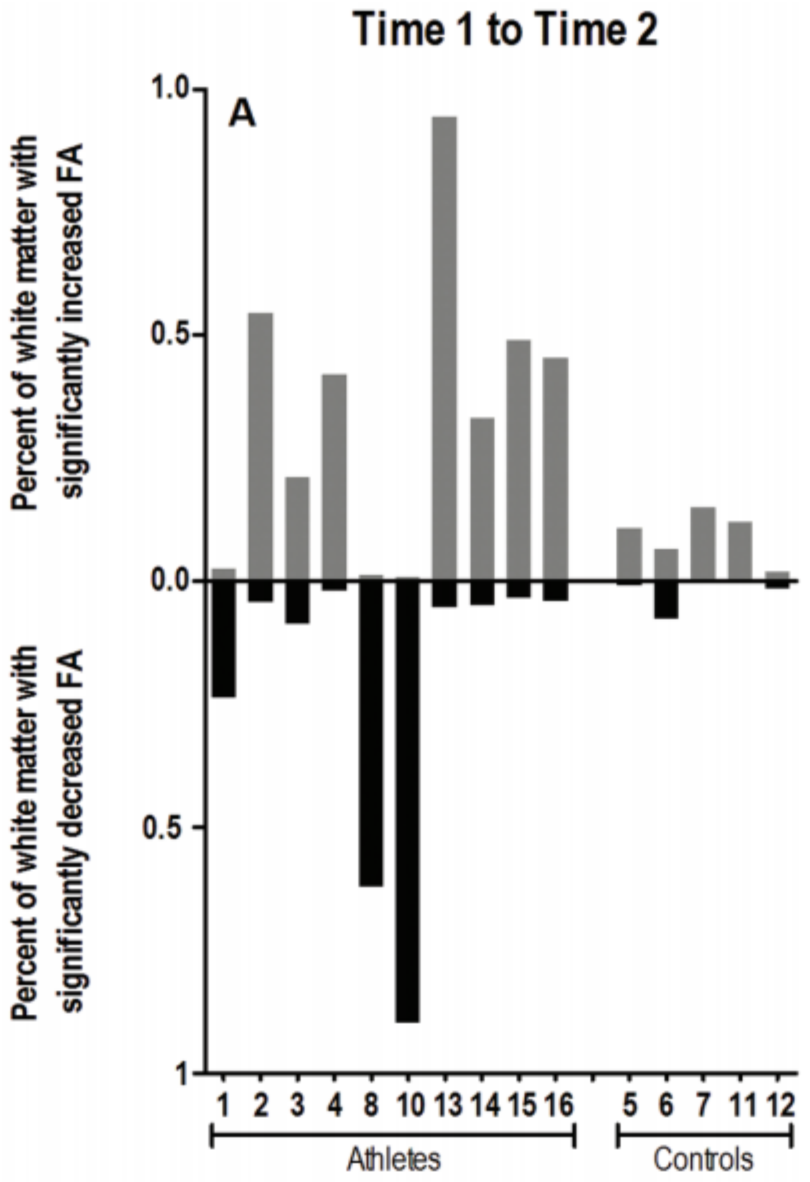
Time 1 to Time 2
A
Percent of white matter with significantly increased FA
Percent of white matter with significantly decreased FA
1.0
0.5
0.0
0.5
1
1 2 3 4 8 10 13 14 15 16
5 6 7 11 12
Athletes
Controls

Modeling the cumulative effect of successive hits

Weighted impact of (*n*-*j*)-th hit:

$$h_{t_{n-j,d}} + \sum_{i=1}^{n-j-1} h_{t_{n-i,d}} \left(\frac{1}{t_{n-j,d} - t_{n-i,d}} \right)$$

$$CI(M)_{TBH} = \sum_{j=0}^{n-1} \left(h_{t_{n-j,d}} + \sum_{i=1}^{n-j-1} h_{t_{n-i,d}} \left(\frac{1}{t_{n-j,d} - t_{n-i,d}} \right) \right)$$

Modeling the cumulative effect of time until assessment

$$T(d) = \sum_{i=1}^{n} \left(\frac{h_{t_{i,d}}}{\max(t_D - t_d, 1)} \right)$$

$$CI(M)_{TUA} = \sum_{d=1}^{M} \left(\sum_{i=1}^{n} h_{t_{i,d}} \left(\frac{1}{\max(t_D - t_d, 1)} \right) \right)$$

where $t_D \geq t_d$.

The cumulative impact over M days is given by:

$$CI(M)_{TBH+TUA} = \sum_{d=1}^{M}\left(\sum_{j=0}^{n-1}\left(\left(h_{t_{n-j,d}} + \sum_{i=1}^{n-j-1} h_{t_{n-i,d}}\left(\frac{1}{t_{n-j,d} - t_{n-i,d}}\right)\right)\frac{1}{\max(t_D - t_d, 1)}\right)\right)$$

where $t_D \geq t_d$ and $t_D - t_d \leq T(d)$

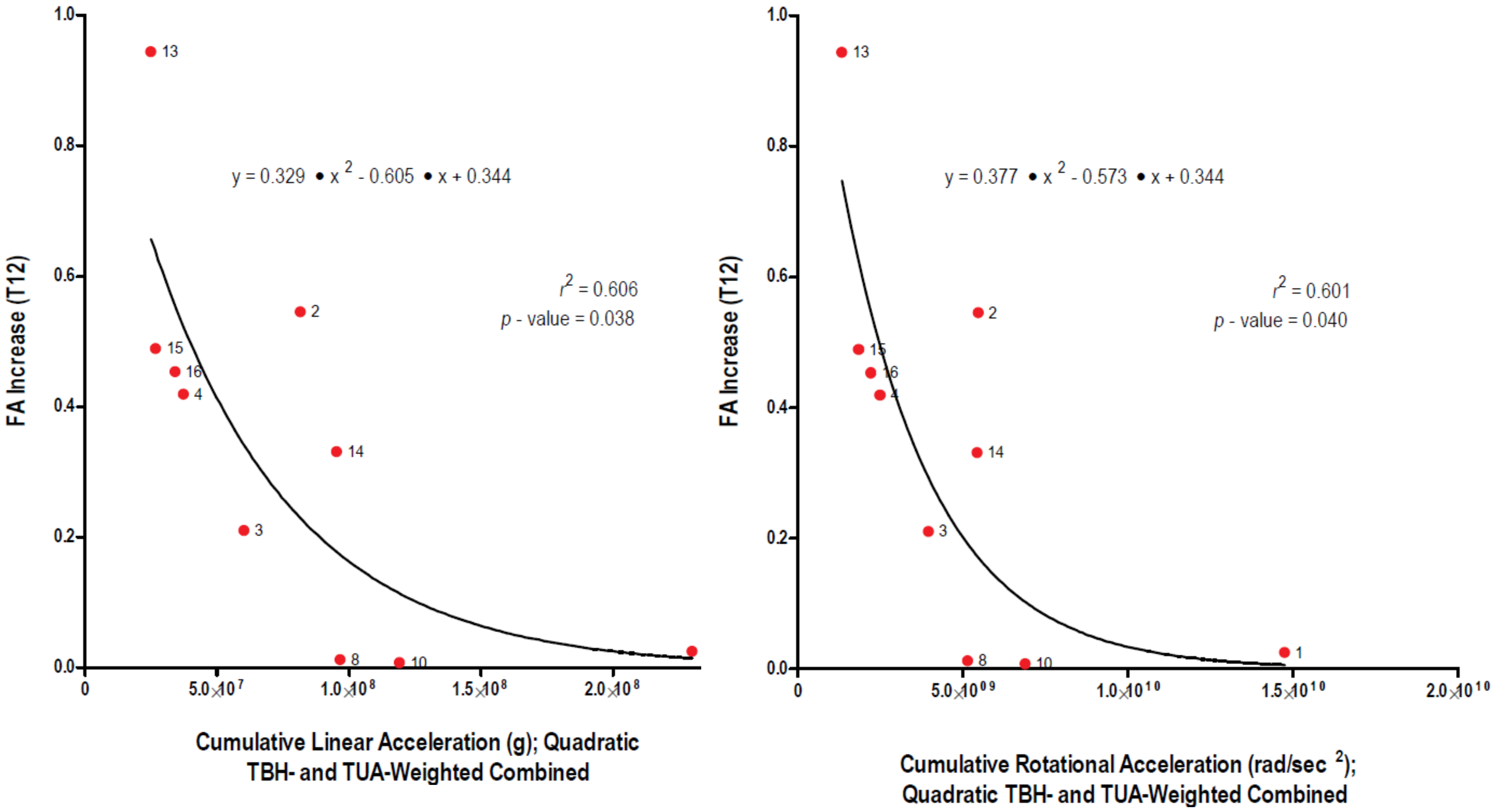

y = 0.329 • x 2 - 0.605 • x + 0.344
r2 = 0.606
p - value = 0.038
FA Increase (T12)
1.0
0.8
0.6
0.4
0.2
0.0
13
2
15
16
4
14
3
8
10
0
5.0×10 7
1.0×10 8
1.5×10 8
2.0×10 8
Cumulative Linear Acceleration (g); Quadratic
TBH- and TUA-Weighted Combined
y = 0.377 • x 2 - 0.573 • x + 0.344
r2 = 0.601
p - value = 0.040
FA Increase (T12)
1.0
0.8
0.6
0.4
0.2
0.0
13
2
15
16
4
14
3
8
10
1
0
5.0×10 9
1.0×10 10
1.5×10 10
2.0×10 10
Cumulative Rotational Acceleration (rad/sec 2);
Quadratic TBH- and TUA-Weighted Combined

Increased fractional anisotropy (FA) is known to be linked to schizophrenia and ADHD. (Li et al. 2010)

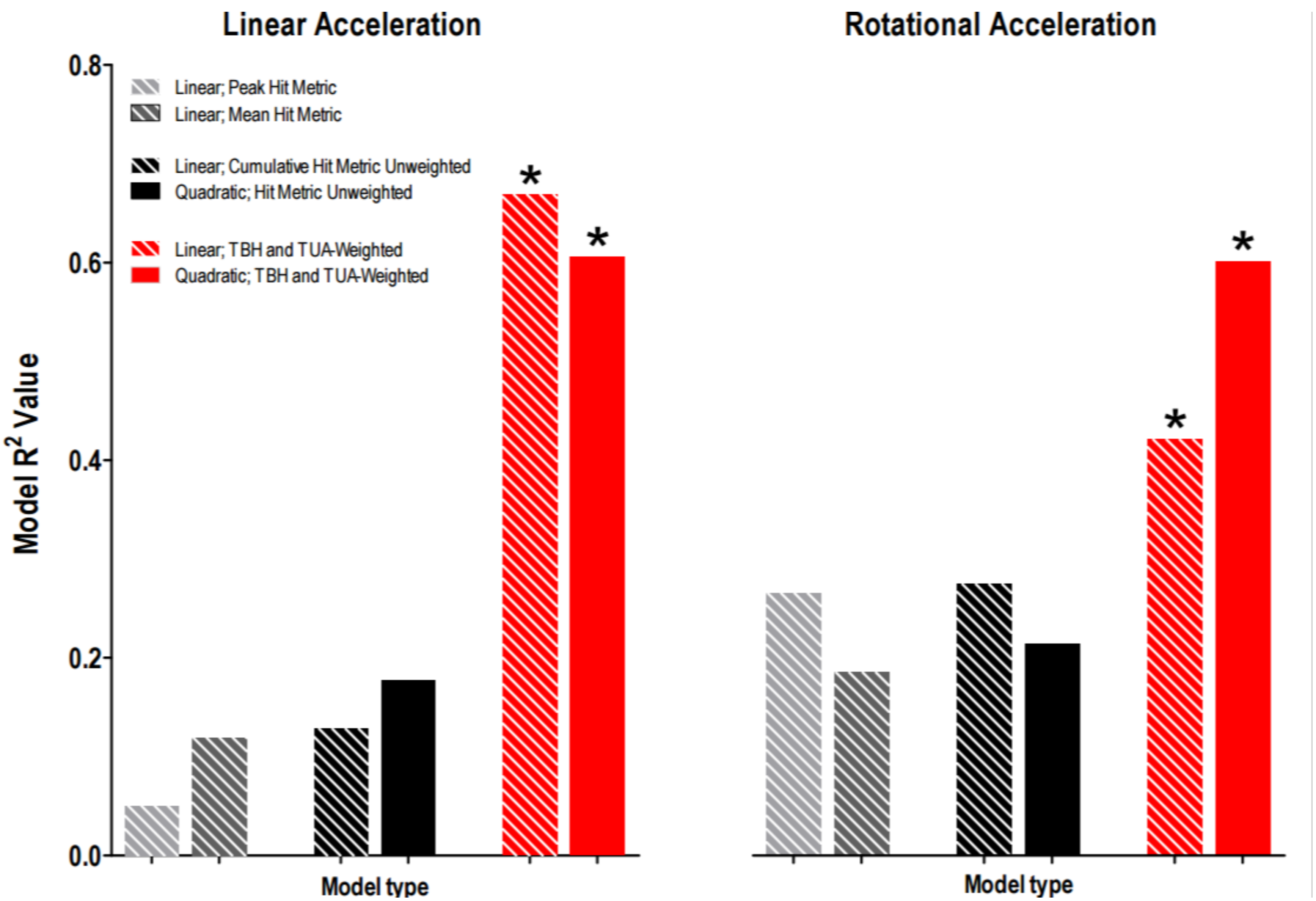

FA Increase	Quadratic; TBH and TUA-Weighted		Quadratic; TBH and TUA-Weighted	
	R	*p* - value	R^2	*p* - value
LA	0.778	0.038	0.606	0.038
RA	0.775	0.040	0.601	0.040
HIC15	0.837	0.015	0.701	0.015
GSI	0.851	0.011	0.725	0.011
HITsp	0.724	0.074	0.524	0.074

Annals of Biomedical Engineering (© 2016)
DOI: 10.1007/s10439-016-1680-9

Novel Method of Weighting Cumulative Helmet Impacts Improves Correlation with Brain White Matter Changes After One Football Season of Sub-concussive Head Blows

KIAN MERCHANT-BORNA,[1] PATRICK ASSELIN,[1] DARREN NARAYAN,[2] BEAU ABAR,[1] COURTNEY M. C. JONES,[1] and JEFFREY J. BAZARIAN[1]

[1]Department of Emergency Medicine, University of Rochester School of Medicine and Dentistry, 265 Crittenden Blvd, Box 655C, Rochester, NY 14642, USA; and [2]School of Mathematical Sciences, Rochester Institute of Technology, Rochester, NY, USA

(*Received 26 October 2015; accepted 14 June 2016*)

Using graph theory to assess efficiency in transportation network design

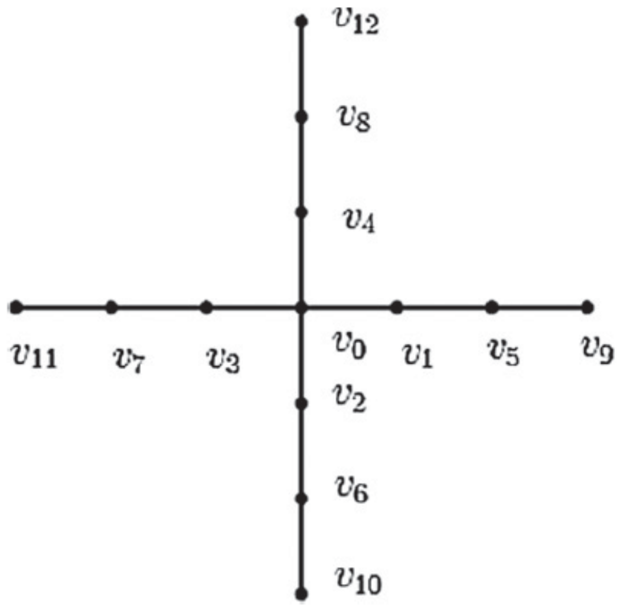

Fig. 2. The subdivided star $S_{4,3}$.

Example 1. Let $G = P_7$ with vertices A, B, C, D, E, F and G.

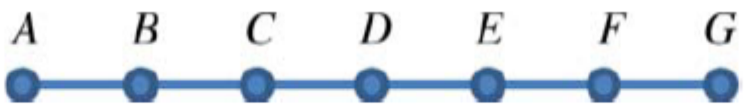

The distances between each pair of vertices are given in the matrix shown below:

$DM =$

$L(G)$	A	B	C	D	E	F	G
A	0	1	2	3	4	5	6
B	1	0	1	2	3	4	5
C	2	1	0	1	2	3	4
D	3	2	1	0	1	2	3
E	4	3	2	1	0	1	2
F	5	4	3	2	1	0	1
G	6	5	4	3	2	1	0

The efficiency matrix is then as follows:

$EM =$

$E(G)$	A	B	C	D	E	F	G
A	0	1	$\frac{1}{2}$	$\frac{1}{3}$	$\frac{1}{4}$	$\frac{1}{5}$	$\frac{1}{6}$
B	1	0	1	$\frac{1}{2}$	$\frac{1}{3}$	$\frac{1}{4}$	$\frac{1}{5}$
C	$\frac{1}{2}$	1	0	1	$\frac{1}{2}$	$\frac{1}{3}$	$\frac{1}{4}$
D	$\frac{1}{3}$	$\frac{1}{2}$	1	0	1	$\frac{1}{2}$	$\frac{1}{3}$
E	$\frac{1}{4}$	$\frac{1}{3}$	$\frac{1}{2}$	1	0	1	$\frac{1}{2}$
F	$\frac{1}{5}$	$\frac{1}{4}$	$\frac{1}{3}$	$\frac{1}{2}$	1	0	1
G	$\frac{1}{6}$	$\frac{1}{5}$	$\frac{1}{4}$	$\frac{1}{3}$	$\frac{1}{2}$	1	0

“Euclidean Efficiency”

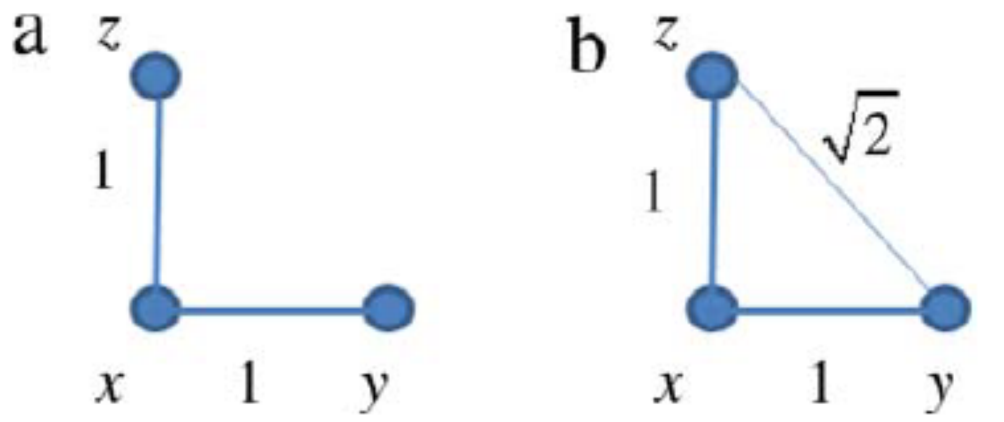

Fig. 1. Comparison of unweighted efficiency (a) and weighted efficiency (b).

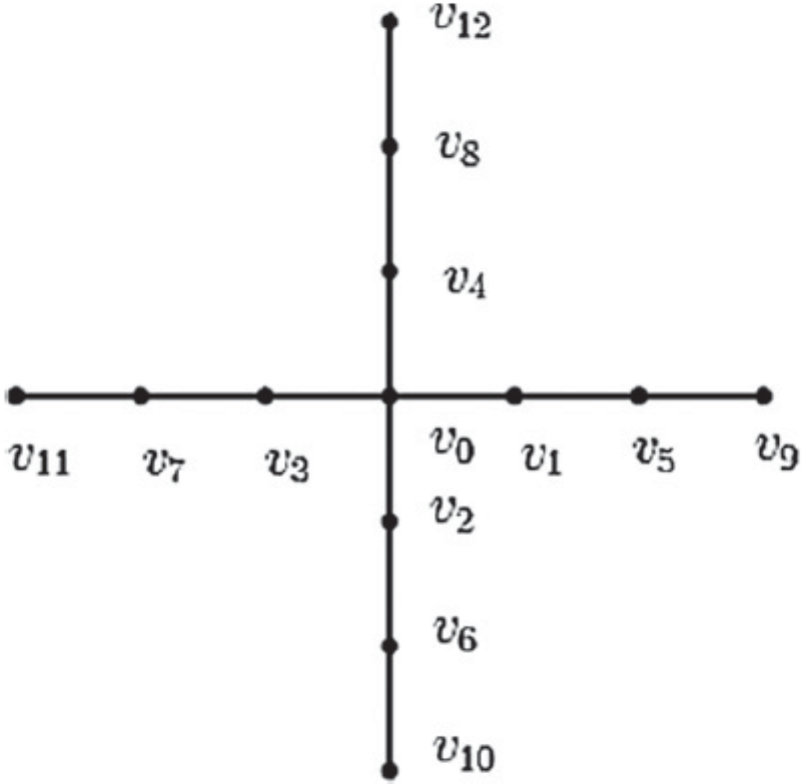

Fig. 2. The subdivided star $S_{4,3}$.

	v_0	v_1	v_2	v_3	v_4	v_5	v_6	v_7	v_8	v_9	v_{10}	v_{11}	v_{12}
v_0	0	1	1	1	1	$\frac{1}{2}$	$\frac{1}{2}$	$\frac{1}{2}$	$\frac{1}{2}$	$\frac{1}{3}$	$\frac{1}{3}$	$\frac{1}{3}$	$\frac{1}{3}$
v_1		0	$\frac{1}{2}$	$\frac{1}{2}$	$\frac{1}{2}$	1	$\frac{1}{3}$	$\frac{1}{3}$	$\frac{1}{3}$	$\frac{1}{2}$	$\frac{1}{4}$	$\frac{1}{4}$	$\frac{1}{4}$
v_2			0	$\frac{1}{2}$	$\frac{1}{2}$	$\frac{1}{3}$	1	$\frac{1}{3}$	$\frac{1}{3}$	$\frac{1}{4}$	$\frac{1}{2}$	$\frac{1}{4}$	$\frac{1}{4}$
v_3				0	$\frac{1}{2}$	$\frac{1}{3}$	$\frac{1}{3}$	1	$\frac{1}{3}$	$\frac{1}{4}$	$\frac{1}{4}$	$\frac{1}{2}$	$\frac{1}{4}$
v_4					0	$\frac{1}{3}$	$\frac{1}{3}$	$\frac{1}{3}$	1	$\frac{1}{4}$	$\frac{1}{4}$	$\frac{1}{4}$	$\frac{1}{2}$
v_5						0	$\frac{1}{4}$	$\frac{1}{4}$	$\frac{1}{4}$	1	$\frac{1}{5}$	$\frac{1}{5}$	$\frac{1}{5}$
v_6							0	$\frac{1}{4}$	$\frac{1}{4}$	$\frac{1}{5}$	1	$\frac{1}{5}$	$\frac{1}{5}$
v_7								0	$\frac{1}{4}$	$\frac{1}{5}$	$\frac{1}{5}$	1	$\frac{1}{5}$
v_8									0	$\frac{1}{5}$	$\frac{1}{5}$	$\frac{1}{5}$	1
v_9										0	$\frac{1}{6}$	$\frac{1}{6}$	$\frac{1}{6}$
v_{10}											0	$\frac{1}{6}$	$\frac{1}{6}$
v_{11}												0	$\frac{1}{6}$
v_{12}													0

Fig. 3. Efficiency matrix for $S_{4,3}$.

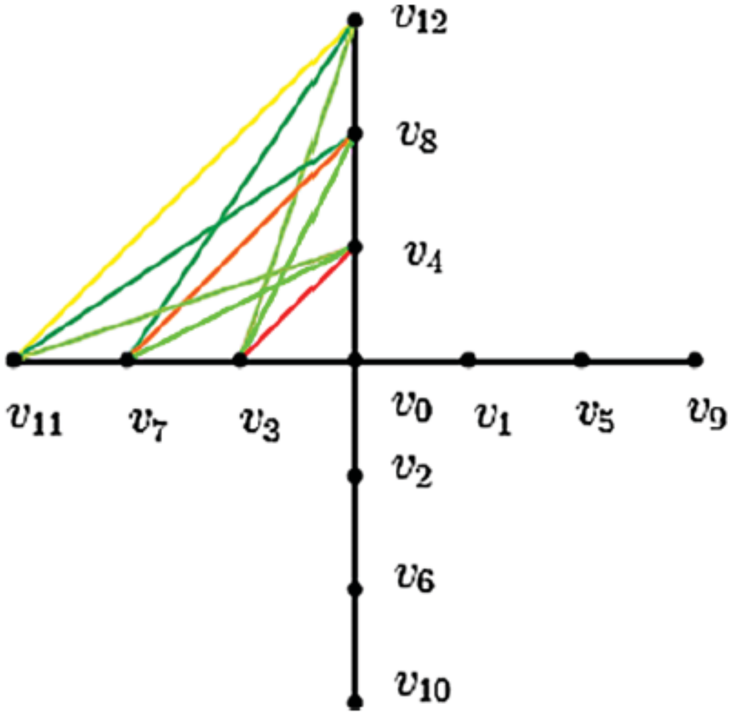

Fig. 4. $S_{4,3}$ with some of the Euclidean distances drawn.

			$j=1$				$j=2$				$j=3$			
		v_0	v_1	v_2	v_3	v_4	v_5	v_6	v_7	v_8	v_9	v_{10}	v_{11}	v_{12}
	v_0	0	1	1	1	1	$\frac{1}{2}$	$\frac{1}{2}$	$\frac{1}{2}$	$\frac{1}{2}$	$\frac{1}{3}$	$\frac{1}{3}$	$\frac{1}{3}$	$\frac{1}{3}$
i=1	v_1	1	0	$\frac{1}{\sqrt{2}}$	$\frac{1}{2}$	$\frac{1}{\sqrt{2}}$	1	$\frac{1}{\sqrt{5}}$	$\frac{1}{3}$	$\frac{1}{\sqrt{5}}$	$\frac{1}{2}$	$\frac{1}{\sqrt{10}}$	$\frac{1}{4}$	$\frac{1}{\sqrt{10}}$
	v_2	1	$\frac{1}{\sqrt{2}}$	0	$\frac{1}{\sqrt{2}}$	$\frac{1}{2}$	$\frac{1}{\sqrt{5}}$	1	$\frac{1}{\sqrt{5}}$	$\frac{1}{3}$	$\frac{1}{\sqrt{10}}$	$\frac{1}{2}$	$\frac{1}{\sqrt{10}}$	$\frac{1}{4}$
	v_3	1	$\frac{1}{2}$	$\frac{1}{\sqrt{2}}$	0	$\frac{1}{\sqrt{2}}$	$\frac{1}{3}$	$\frac{1}{\sqrt{5}}$	1	$\frac{1}{\sqrt{5}}$	$\frac{1}{4}$	$\frac{1}{\sqrt{10}}$	$\frac{1}{2}$	$\frac{1}{\sqrt{10}}$
	v_4	1	$\frac{1}{\sqrt{2}}$	$\frac{1}{2}$	$\frac{1}{\sqrt{2}}$	0	$\frac{1}{\sqrt{5}}$	$\frac{1}{3}$	$\frac{1}{\sqrt{5}}$	1	$\frac{1}{\sqrt{10}}$	$\frac{1}{4}$	$\frac{1}{\sqrt{10}}$	$\frac{1}{2}$
i=2	v_5	$\frac{1}{2}$	1	$\frac{1}{\sqrt{5}}$	$\frac{1}{3}$	$\frac{1}{\sqrt{5}}$	0	$\frac{1}{\sqrt{8}}$	$\frac{1}{4}$	$\frac{1}{\sqrt{8}}$	1	$\frac{1}{\sqrt{13}}$	$\frac{1}{5}$	$\frac{1}{\sqrt{13}}$
	v_6	$\frac{1}{2}$	$\frac{1}{\sqrt{5}}$	1	$\frac{1}{\sqrt{5}}$	$\frac{1}{3}$	$\frac{1}{\sqrt{8}}$	0	$\frac{1}{\sqrt{8}}$	$\frac{1}{4}$	$\frac{1}{\sqrt{13}}$	1	$\frac{1}{\sqrt{13}}$	$\frac{1}{5}$
	v_7	$\frac{1}{2}$	$\frac{1}{3}$	$\frac{1}{\sqrt{5}}$	1	$\frac{1}{\sqrt{5}}$	$\frac{1}{4}$	$\frac{1}{\sqrt{8}}$	0	$\frac{1}{\sqrt{8}}$	$\frac{1}{5}$	$\frac{1}{\sqrt{13}}$	1	$\frac{1}{\sqrt{13}}$
	v_8	$\frac{1}{2}$	$\frac{1}{\sqrt{5}}$	$\frac{1}{3}$	$\frac{1}{\sqrt{5}}$	1	$\frac{1}{\sqrt{8}}$	$\frac{1}{4}$	$\frac{1}{\sqrt{8}}$	0	$\frac{1}{\sqrt{13}}$	$\frac{1}{5}$	$\frac{1}{\sqrt{13}}$	1
i=3	v_9	$\frac{1}{3}$	$\frac{1}{2}$	$\frac{1}{\sqrt{10}}$	$\frac{1}{4}$	$\frac{1}{\sqrt{10}}$	1	$\frac{1}{\sqrt{13}}$	$\frac{1}{5}$	$\frac{1}{\sqrt{13}}$	0	$\frac{1}{\sqrt{18}}$	$\frac{1}{6}$	$\frac{1}{\sqrt{18}}$
	v_{10}	$\frac{1}{3}$	$\frac{1}{\sqrt{10}}$	$\frac{1}{2}$	$\frac{1}{\sqrt{10}}$	$\frac{1}{4}$	$\frac{1}{\sqrt{13}}$	1	$\frac{1}{\sqrt{13}}$	$\frac{1}{5}$	$\frac{1}{\sqrt{18}}$	0	$\frac{1}{\sqrt{18}}$	$\frac{1}{6}$
	v_{11}	$\frac{1}{3}$	$\frac{1}{4}$	$\frac{1}{\sqrt{10}}$	$\frac{1}{2}$	$\frac{1}{\sqrt{10}}$	$\frac{1}{5}$	$\frac{1}{\sqrt{13}}$	1	$\frac{1}{\sqrt{13}}$	$\frac{1}{6}$	$\frac{1}{\sqrt{18}}$	0	$\frac{1}{\sqrt{18}}$
	v_{12}	$\frac{1}{3}$	$\frac{1}{\sqrt{10}}$	$\frac{1}{4}$	$\frac{1}{\sqrt{10}}$	$\frac{1}{2}$	$\frac{1}{\sqrt{13}}$	$\frac{1}{5}$	$\frac{1}{\sqrt{13}}$	1	$\frac{1}{\sqrt{18}}$	$\frac{1}{6}$	$\frac{1}{\sqrt{18}}$	0

Fig. 5. Euclidean efficiency matrix for $S_{4,3}$.

* This has both theoretical and applied extensions.

Metropolitan Atlanta Rapid Transit Authority (MARTA)

How efficient is the network compared to a network where every pair of stations is connected by a direct line?

To answer this question what data would we need?

Rail distances (provided by MARTA)

	NS	SS	D	MC	BH	LC	LNX	BHOG	CH	DRA	Arts	MT	NA	CVC	PCH	5PT	GS	K	I	EW	EL	DCT	AVD	KNS	IND	GNT	WE	OAK	LW	EP	COL	APT	DOME	VC	ASH	WL	HAM	BNK	
NS	0	1.1	2	3	7.7	9.9	11.8	13.3	16	18	13.1	13.6	14.2	14.6	15.1	15.6	16	16.7	18.1	18.9	20.6	21.9	22.7	24.6	25.9	16	17.5	19	20.1	22	23.8	24.6	16	16.4	17.1	18.8	20.3	18.5	NS
SS		0	0.9	1.9	6.6	8.8	10.7	12.2	14.9	16.9	12	12.5	13.1	13.5	14	14.5	14.9	15.6	17	17.8	19.5	20.8	21.6	23.5	24.8	14.9	16.4	17.9	19	20.9	22.7	23.5	14.9	15.3	16	17.7	19.2	17.4	SS
D			0	1	5.7	7.9	9.8	11.3	14	16	11.1	11.6	12.2	12.6	13.1	13.6	14	14.7	16.1	16.9	18.6	19.9	20.7	22.6	23.9	14	15.5	17	18.1	20	21.8	22.6	14	14.4	15.1	16.8	18.3	16.5	D
MC				0	4.7	6.9	8.8	10.3	13	15	10.1	10.6	11.2	11.6	12.1	12.6	13	13.7	15.1	15.9	17.6	18.9	19.7	21.6	22.9	13	14.5	16	17.1	19	20.8	21.6	13	13.4	14.1	15.8	17.3	15.5	MC
BH					0	2.2	4.1	5.6	8.3	10.3	5.4	5.9	6.5	6.9	7.4	7.9	8.3	9	10.4	11.2	12.9	14.2	15	16.9	18.2	8.3	9.8	11.3	12.4	14.3	16.1	16.9	8.3	8.7	9.4	11.1	12.6	10.8	BH
LC						0	1.9	3.4	6.1	8.1	3.2	3.7	4.3	4.7	5.2	5.7	6.1	6.8	8.2	9	10.7	12	12.8	14.7	16	6.1	7.6	9.1	10.2	12.1	13.9	14.7	6.1	6.5	7.2	8.9	10.4	8.6	LC
LNX							0	1.5	4.2	6.2	5.1	5.6	6.2	6.6	7.1	7.6	8	8.7	10.1	10.9	12.6	13.9	14.7	16.6	17.9	8	9.5	11	12.1	14	15.8	16.6	8	8.4	9.1	10.8	12.3	10.5	LNX
BHOG								0	2.7	4.7	6.6	7.1	7.7	8.1	8.6	9.1	9.5	10.2	11.6	12.4	14.1	15.4	16.2	18.1	19.4	9.5	11	12.5	13.6	15.5	17.3	18.1	9.5	9.9	10.6	12.3	13.8	12	BHOG
CH									0	2	9.3	9.8	10.4	10.8	11.3	11.8	12.2	12.9	14.3	15.1	16.8	18.1	18.9	20.8	22.1	12.2	13.7	15.2	16.3	18.2	20	20.8	12.2	12.6	13.3	15	16.5	14.7	CH
DRA										0	11.3	11.8	12.4	12.8	13.3	13.8	14.2	14.9	16.3	17.1	18.8	20.1	20.9	22.8	24.1	14.2	15.7	17.2	18.3	20.2	22	22.8	14.2	14.6	15.3	17	18.5	16.7	DRA
ARTS											0	0.5	1.1	1.5	2	2.5	2.9	3.6	5	5.8	7.5	8.8	9.6	11.5	12.8	2.9	4.4	5.9	7	8.9	10.7	11.5	2.9	3.3	4	5.7	7.2	5.4	ARTS
MT												0	0.6	1	1.5	2	2.4	3.1	4.5	5.3	7	8.3	9.1	11	12.3	2.4	3.9	5.4	6.5	8.4	10.2	11	2.4	2.8	3.5	5.2	6.7	4.9	MT
NA													0	0.6	0.9	1.4	1.8	2.5	3.9	4.7	6.4	7.7	8.5	10.4	11.7	1.8	3.3	4.8	5.9	7.8	9.6	10.4	1.8	2.2	2.9	4.6	6.1	4.3	NA
CVC														0	0.5	1	1.4	2.1	3.5	4.3	6	7.3	8.1	10	11.3	1.4	2.9	4.4	5.5	7.4	9.2	10	1.4	1.8	2.5	4.2	5.7	3.9	CVC
PCH															0	0.5	0.9	1.6	3	3.8	5.5	6.8	7.6	9.5	10.8	0.9	2.4	3.9	5	6.9	8.7	9.5	0.9	1.3	2	3.7	5.2	3.4	PCH
5PT																0	0.4	1.1	2.5	3.3	5	6.3	7.1	9	10.3	0.4	1.9	3.4	4.5	6.4	8.2	9	0.4	0.8	1.5	3.2	4.7	2.9	5PT
GS																	0	0.7	2.1	2.9	4.6	5.9	6.7	8.6	9.9	0.8	2.3	3.8	4.9	6.8	8.6	9.4	0.8	1.2	1.9	3.6	5.1	3.3	GS
K																		0	1.4	2.2	3.9	5.2	6	7.9	9.2	1.5	3	4.5	5.6	7.5	9.3	10.1	1.5	1.9	2.6	4.3	5.8	4	K
I																			0	0.8	2.5	3.8	4.6	6.5	7.8	2.9	4.4	5.9	7	8.9	10.7	11.5	2.9	3.3	4	5.7	7.2	5.4	I
EW																				0	1.7	3	3.8	5.7	7	3.7	5.2	6.7	7.8	9.7	11.5	12.3	3.7	4.1	4.8	6.5	8	6.2	EW
EL																					0	1.3	2.1	4	5.3	5.4	6.9	8.4	9.5	11.4	13.2	14	5.4	5.8	6.5	8.2	9.7	7.9	EL
DCT																						0	0.8	2.7	4	6.7	8.2	9.7	10.8	12.7	14.5	15.3	6.7	7.1	7.8	9.5	11	9.2	DCT
AVD																							0	1.9	3.2	7.5	9	10.5	11.6	13.5	15.3	16.1	7.5	7.9	8.6	10.3	11.8	10	AVD
KNS																								0	1.3	9.4	10.9	12.4	13.5	15.4	17.2	18	9.4	9.8	10.5	12.2	13.7	11.9	KNS
IC																									0	10.7	12.2	13.7	14.8	16.7	18.5	19.3	10.7	11.1	11.8	13.5	15	13.2	IC
GNT																										0	1.5	3	4.1	6	7.8	8.6	0.8	1.2	1.9	3.6	5.1	3.3	GNT
WE																											0	1.5	2.6	4.5	6.3	7.1	2.3	2.7	3.4	5.1	6.6	4.8	WE
OAK																												0	1.1	3	4.8	5.6	3.8	4.2	4.9	6.6	8.1	6.3	OAK
LW																													0	1.9	3.7	4.5	4.9	5.3	6	7.7	9.2	7.4	LW
EP																														0	1.8	2.6	6.8	7.2	7.9	9.6	11.1	9.3	EP
COL																															0	0.8	8.6	9	9.7	11.4	12.9	11.1	COL
APT																																0	9.4	9.8	10.5	12.2	13.7	11.9	APT
DOME																																	0	0.4	1.1	2.8	4.3	2.5	DOME
VC																																		0	0.7	2.4	3.9	2.1	VC
ASH																																			0	1.7	3.2	1.4	ASH
WL																																				0	1.5	3.1	WL
HAM																																					0	4.6	HAM
BNK																																						0	BNK
	NS	SS	D	MC	BH	LC	LNX	BHOG	CH	DRA	Arts	MT	NA	CVC	PCH	5PT	GS	K	I	EW	EL	DCT	AVD	KNS	IND	GNT	WE	OAK	LW	EP	COL	APT	DOME	VC	ASH	WL	HAM	BNK	

Using Google Earth we determined the Euclidean distance between every pair of stations.

	NS	SS	D	MC	BH	LC	LNX	BHOG	CH	DRA	Arts	MT	NA	CVC	PCH	SPT	GS	K	I	EW	EL	DCT	AVD	KNS	IND	GNT	WE	OAK	LW	EP	COL	APT	DOME	VC	ASH	WL	HAM	BNK	
NS	0	1.1	2	3	7.7	9.9	11.8	13.3	16	18	13.1	13.1	13.7	14.1	14.6	15.1	15.5	16.2	17.6	18.4	20.1	21.4	22.2	24.1	25.4	15.5	17	18.5	19.6	21.5	23.3	24.1	15.5	15.9	16.6	18.3	19.8	18	NS
SS		0	0.9	1.9	6.6	8.8	10.7	12.2	14.9	16.9	12	12	12.6	13	13.5	14	14.4	15.1	16.5	17.3	19	20.3	21.1	23	24.3	14.4	15.9	17.4	18.5	20.4	22.2	23	14.4	14.8	15.5	17.2	18.7	16.9	SS
D			0	1	5.7	7.9	9.8	11.3	14	16	11.1	11.1	11.7	12.1	12.6	13.1	13.5	14.2	15.6	16.4	18.1	19.4	20.2	22.1	23.4	13.5	15	16.5	17.6	19.5	21.3	22.1	13.5	13.9	14.6	16.3	17.8	16	D
MC				0	4.7	6.9	8.8	10.3	13	15	10.1	10.1	10.7	11.1	11.6	12.1	12.5	13.2	14.6	15.4	17.1	18.4	19.2	21.1	22.4	12.5	14	15.5	16.6	18.5	20.3	21.1	12.5	12.9	13.6	15.3	16.8	15	MC
BH					0	2.2	4.1	5.6	8.3	10.3	5.4	5.4	6	6.4	6.9	7.4	7.8	8.5	9.9	10.7	12.4	13.7	14.5	16.4	17.7	7.8	9.3	10.8	11.9	13.8	15.6	16.4	7.8	8.2	8.9	10.6	12.1	10.3	BH
LC						0	1.9	3.4	6.1	8.1	3.2	3.7	4.3	4.7	5.2	5.7	6.1	6.8	8.2	9	10.7	12	12.8	14.7	16	6.1	7.6	9.1	10.2	12.1	13.9	14.7	6.1	6.5	7.2	8.9	10.4	8.6	LC
LNX							0	1.5	4.2	6.2	5.1	5.1	5.7	6.1	6.6	7.1	7.5	8.2	9.6	10.4	12.1	13.4	14.2	16.1	17.4	7.5	9	10.5	11.6	13.5	15.3	16.1	7.5	7.9	8.6	10.3	11.8	10	LNX
BHOG								0	2.7	4.7	6.6	6.6	7.2	7.6	8.1	8.6	9	9.7	11.1	11.9	13.6	14.9	15.7	17.6	18.9	9	10.5	12	13.1	15	16.8	17.6	9	9.4	10.1	11.8	13.3	11.5	BHOG
CH									0	2	9.3	9.3	9.9	10.3	10.8	11.3	11.7	12.4	13.8	14.6	16.3	17.6	18.4	20.3	21.6	11.7	13.2	14.7	15.8	17.7	19.5	20.3	11.7	12.1	12.8	14.5	16	14.2	CH
DRA										0	11.3	11.3	11.9	12.3	12.8	13.3	13.7	14.4	15.8	16.6	18.3	19.6	20.4	22.3	23.6	13.7	15.2	16.7	17.8	19.7	21.5	22.3	13.7	14.1	14.8	16.5	18	16.2	DRA
ARTS											0	0.5	1.1	1.5	2	2.5	2.9	3.6	5	5.8	7.5	8.8	9.6	11.5	12.8	2.9	4.4	5.9	7	8.9	10.7	11.5	2.9	3.3	4	5.7	7.2	5.4	ARTS
MT												0	0.6	1	1.5	2	2.4	3.1	4.5	5.3	7	8.3	9.1	11	12.3	2.4	3.9	5.4	6.5	8.4	10.2	11	2.4	2.8	3.5	5.2	6.7	4.9	MT
NA													0	0.6	0.9	1.4	1.8	2.5	3.9	4.7	6.4	7.7	8.5	10.4	11.7	1.8	3.3	4.8	5.9	7.8	9.6	10.4	1.8	2.2	2.9	4.6	6.1	4.3	NA
CVC														0	0.5	1	1.4	2.1	3.5	4.3	6	7.3	8.1	10	11.3	1.4	2.9	4.4	5.5	7.4	9.2	10	1.4	1.8	2.5	4.2	5.7	3.9	CVC
PCH															0	0.5	0.9	1.6	3	3.8	5.5	6.8	7.6	9.5	10.8	0.9	2.4	3.9	5	6.9	8.7	9.5	0.9	1.3	2	3.7	5.2	3.4	PCH
SPT																0	0.4	1.1	2.5	3.3	5	6.3	7.1	9	10.3	0.4	1.9	3.4	4.5	6.4	8.2	9	0.4	0.8	1.5	3.2	4.7	2.9	SPT
GS																	0	0.7	2.1	2.9	4.6	5.9	6.7	8.6	9.9	0.8	2.3	3.8	4.9	6.8	8.6	9.4	0.8	1.2	1.9	3.6	5.1	3.3	GS
K																		0	1.4	2.2	3.9	5.2	6	7.9	9.2	1.5	3	4.5	5.6	7.5	9.3	10.1	1.5	1.9	2.6	4.3	5.8	4	K
I																			0	0.8	2.5	3.8	4.6	6.5	7.8	2.9	4.4	5.9	7	8.9	10.7	11.5	2.9	3.3	4	5.7	7.2	5.4	I
EW																				0	1.7	3	3.8	5.7	7	3.7	5.2	6.7	7.8	9.7	11.5	12.3	3.7	4.1	4.8	6.5	8	6.2	EW
EL																					0	1.3	2.1	4	5.3	5.4	6.9	8.4	9.5	11.4	13.2	14	5.4	5.8	6.5	8.2	9.7	7.9	EL
DCT																						0	0.8	2.7	4	6.7	8.2	9.7	10.8	12.7	14.5	15.3	6.7	7.1	7.8	9.5	11	9.2	DCT
AVD																							0	1.9	3.2	7.5	9	10.5	11.6	13.5	15.3	16.1	7.5	7.9	8.6	10.3	11.8	10	AVD
KNS																								0	1.3	9.4	10.9	12.4	13.5	15.4	17.2	18	9.4	9.8	10.5	12.2	13.7	11.9	KNS
IC																									0	10.7	12.2	13.7	14.8	16.7	18.5	19.3	10.7	11.1	11.8	13.5	15	13.2	IC
GNT																										0	1.5	3	4.1	6	7.8	8.6	0.8	1.2	1.9	3.6	5.1	3.3	GNT
WE																											0	1.5	2.6	4.5	6.3	7.1	2.3	2.7	3.4	5.1	6.6	4.8	WE
OAK																												0	1.1	3	4.8	5.6	3.8	4.2	4.9	6.6	8.1	6.3	OAK
LW																													0	1.9	3.7	4.5	4.9	5.3	6	7.7	9.2	7.4	LW
EP																														0	1.8	2.6	6.8	7.2	7.9	9.6	11.1	9.3	EP
COL																															0	0.8	8.6	9	9.7	11.4	12.9	11.1	COL
APT																																0	9.4	9.8	10.5	12.2	13.7	11.9	APT
DOME																																	0	0.4	1.1	2.8	4.3	2.5	DOME
VC																																		0	0.7	2.4	3.9	2.1	VC
ASH																																			0	1.7	3.2	1.4	ASH
WL																																				0	1.5	3.1	WL
HAM																																					0	4.6	HAM
BNK																																						0	BNK
	NS	SS	D	MC	BH	LC	LNX	BHOG	CH	DRA	Arts	MT	NA	CVC	PCH	SPT	GS	K	I	EW	EL	DCT	AVD	KNS	IND	GNT	WE	OAK	LW	EP	COL	APT	DOME	VC	ASH	WL	HAM	BNK	

$$E_{Ratio}(\text{MARTA}) = \frac{311.7036}{379.8169} = 0.8207.$$

The MARTA network is 82% as efficient as a network where each pair of stations is connected by a direct line.

Contents lists available at ScienceDirect

Physica A

journal homepage: www.elsevier.com/locate/physa

Efficiency of star-like graphs and the Atlanta subway network

Bryan Ek[a], Caitlin VerSchneider[b], Darren A. Narayan[a,*]

[a] School of Mathematical Sciences, Rochester Institute of Technology, Rochester, NY 14623, United States

[b] Mathematics Department, Nazareth College, Rochester, NY 14618, United States

STEM Real World Applications of Mathematics
(NSF-CCLI Grant #1019532)

Joy Lind
University of Sioux Falls
joy.lind@usiouxfalls.edu

Darren Narayan
Rochester Institute of Technology
dansma@rit.edu

We have developed a library of modules with real world applications of graph theory.

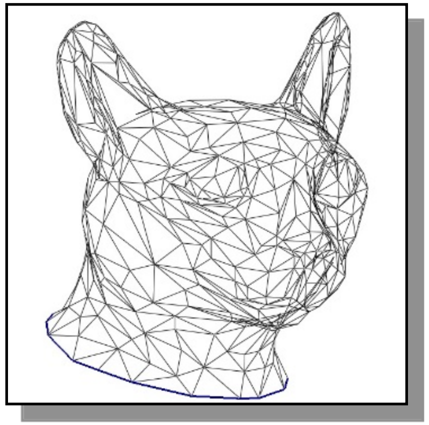

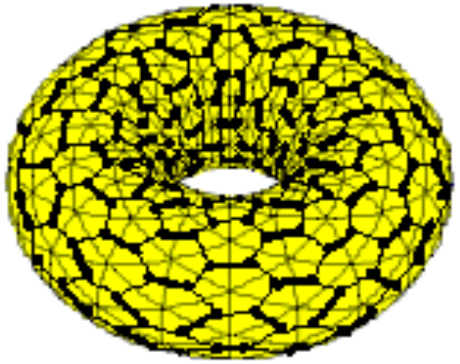

- Measuring Brain Connectivity (Rochester Center for Brain Imaging)
- 3-D Surface Reconstruction (Microsoft Research)
- Eulerian Digraphs (Tuition Exchange Network)
- Enumerating Spanning Trees (Cisco Systems)
- Minimum weight spanning trees (National LambdaRail)
- Distance, diameter, radius, and eccentricity (jetBlue Airways)
- Menger's Theorem (National LambdaRail)

Wanted: Beta – testers!

Mathematical Modeling Ph.D Program

Starts Fall 2017

For information contact Dr. Elizabeth Cherry, excsma@rit.edu

Thank you for your time!